A basal ganglia-like cortical–amygdalar–hypothalamic network mediates feeding behavior

Marie Barbier[a,1,2], Sandrine Chometton[b], Arnaud Pautrat[c], Carole Miguet-Alfonsi[a], Frédérique Datiche[d], Jean Gascuel[d], Dominique Fellmann[a], Yvan Peterschmitt[a], Véronique Coizet[c], and Pierre-Yves Risold[a]

[a]Neurosciences Intégratives et Cliniques EA481, Université de Bourgogne Franche-Comté, 25000 Besançon, France; [b]Department of Biological Sciences, University of Southern California, Los Angeles, CA 90089-0371; [c]INSERM, Grenoble Institute of Neurosciences, Université Grenoble Alpes, F38000 Grenoble, France; and [d]Centre des Sciences du Goût et de l'Alimentation, Unité Mixte de Recherche CNRS, Institut National de la Recherche Agronomique, Université de Bourgogne, 21000 Dijon, France

Edited by Peter L. Strick, University of Pittsburgh, Pittsburgh, PA, and approved May 20, 2020 (received for review March 19, 2020)

The insular cortex (INS) is extensively connected to the central nucleus of the amygdala (CEA), and both regions send convergent projections into the caudal lateral hypothalamus (LHA) encompassing the parasubthalamic nucleus (PSTN). However, the organization of the network between these structures has not been clearly delineated in the literature, although there has been an upsurge in functional studies related to these structures, especially with regard to the cognitive and psychopathological control of feeding. We conducted tract-tracing experiments from the INS and observed a pathway to the PSTN region that runs parallel to the canonical hyperdirect pathway from the isocortex to the subthalamic nucleus (STN) adjacent to the PSTN. In addition, an indirect pathway with a relay in the central amygdala was also observed that is similar in its structure to the classic indirect pathway of the basal ganglia that also targets the STN. C-Fos experiments showed that the PSTN complex reacts to neophobia and sickness induced by lipopolysaccharide or cisplatin. Chemogenetic (designer receptors exclusively activated by designer drugs [DREADD]) inhibition of tachykininergic neurons (Tac1) in the PSTN revealed that this nucleus gates a stop "no-eat" signal to refrain from feeding when the animal is subjected to sickness or exposed to a previously unknown source of food. Therefore, our anatomical findings in rats and mice indicate that the INS-PSTN network is organized in a similar manner as the hyperdirect and indirect basal ganglia circuitry. Functionally, the PSTN is involved in gating feeding behavior, which is conceptually homologous to the motor no-go response of the adjacent STN.

insular cortex | central amygdala nucleus | hypothalamus | basal ganglia

The voluntary action of feeding depends on multiple factors, including metabolic status, food availability, and palatability. The determining action of these factors on food consumption is gated by additional internal body signals (e.g., pain, infection, inflammation), affective state, and behavioral context. Many interacting brain regions are therefore mobilized. Among them, the insular cortical region (INS) is a key brain area involved in interoception (from gustatory to visceral pain perceptions) and cognition (from emotion to motivation) (1, 2). The INS interacts with other cortical fields, such as the lateral prefrontal and anterior cingulate areas, for higher cognitive processes (3). Descending pathways from the INS to the ventral telencephalon, including the amygdala, and to the brainstem are also of paramount importance in shaping behavioral and emotional outputs (4). However, the organization of these descending pathways still lacks accurate characterization compared to that of adjacent motor or somatosensory cerebral cortical areas. Indeed, the classic basal ganglia network is built upon motor cortical afferents to the striatum, with subsequent direct/indirect pathways from the striatum and pallidum to the substantia nigra (SN) and the subthalamic nucleus (STN) (5, 6) (Fig. 1*A*). This network includes a hyperdirect pathway to the STN from the motor, somatosensory and prefrontal cortical areas that involve or are anatomically linked to the INS (7). The INS lacks a direct projection to the STN, which is a characteristic of the hyperdirect basal ganglia pathway, but projects to ventral striatal structures. Moreover, the INS is tightly connected with the central nucleus of the amygdala (CEA). The CEA is a complex structure in the basal telencephalon and is often included in the striatal compartment based on cytoarchitectural, neurochemical, and hodological resemblances with the caudoputamen nucleus (8). The development of the CEA is also evocative of a striatal nature (9). Anatomical evidence shows that CEA and INS projections converge in a caudal lateral hypothalamic region that includes the parasubthalamic nucleus (PSTN) recently described on the basis of tachykinin-1 gene expression in rodents (10). The PSTN lies adjacent to the STN, and the PSTN projections are also reminiscent of those of the STN (11). Functionally, the PSTN is involved in ingestive behaviors. A robust and very rapid expression of the transcription factor c-Fos, a marker of neuronal activation, is induced in the PSTN by the ingestion of solid palatable food, a sucrose solution or even water in thirsty animals (12), but some authors have suggested that the PSTN may have a role in satiety (13–15).

In the present work, we first analyzed in detail the network connecting the INS, the CEA, and the PSTN in rodents. We then

Significance

The network connecting the insular cortex, the central nucleus of the amygdala, and a caudal hypothalamic nuclear complex including the parasubthalamic nucleus (PSTN) is of interest due to its role in controlling feeding behavior. Here, we show that the organization of this network is similar to that of the basal ganglia network, implying that both fit within a simplified structural plan of the forebrain. Then, we demonstrate that the PSTN complex modulates behavior in response to hedonic factors normally inducing a "reward effect." The PSTN complex is involved in a "non-feed" response equivalent of a "non-reward" evaluation: "I don't want to consume this food, recognized as good, because I am not in a conducive emotional or physiological state."

Author contributions: M.B., Y.P., and P.-Y.R. designed research; M.B., S.C., A.P., C.M.-A., and V.C. performed research; M.B., F.D., J.G., D.F., and P.-Y.R. contributed new reagents/analytic tools; M.B., A.P., V.C., and P.-Y.R. analyzed data; M.B. and P.-Y.R. wrote the paper; and D.F. and Y.P. provided feedback on the manuscript.

The authors declare no competing interest.

This article is a PNAS Direct Submission.

[1]Present addresses: Department of Psychiatry, Icahn School of Medicine at Mount Sinai, New York, NY 10029; and Seaver Autism Center for Research and Treatment, Icahn School of Medicine at Mount Sinai, New York, NY 10029.

[2]To whom correspondence may be addressed. Email: marie.barbier@mssm.edu.

This article contains supporting information online at https://www.pnas.org/lookup/suppl/doi:10.1073/pnas.2004914117/-/DCSupplemental.

First published June 22, 2020.

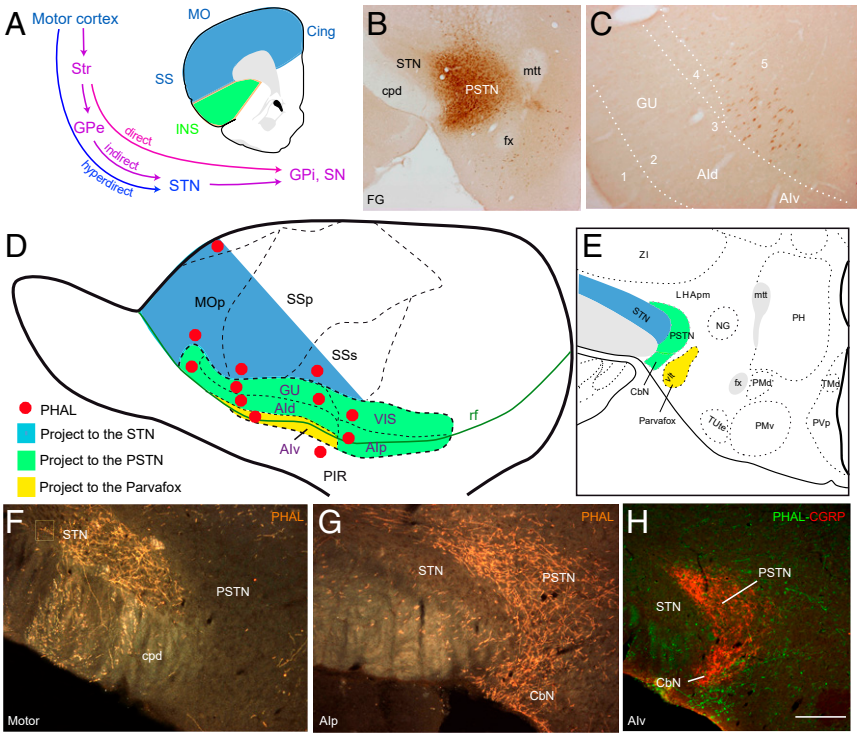

Fig. 1. Projections from the INS to the PSTN region. (*A*) Line drawing that illustrates the organization of the classic basal ganglia network from the motor cortex to the STN that illustrates the hyperdirect, direct, and indirect pathways. (*B* and *C*) Fluorogold injection in the PSTN (*B*) retrogradely labels many cells in layer 5 of the INS (*C*). The majority of these cells are in the AId and AIp. (*D* and *E*) Line drawings illustrating PHAL injection sites in the insular cortex (*D*) and the topographic organization of the projections observed in the STN, PSTN/CbN, and Parvafox regions (*E*). Whereas the isocortex innervates the STN as part of the basal ganglia hyperdirect pathway, the INS innervates the PSTN with the exception of the AIv that targets the CbN and Parvafox nucleus. (*F–H*) Photomicrographs illustrating the innervation of the STN and PSTN/CbN after PHAL injection in the motor cortex (*F*), the AIp (*G*), or the AIv (*H*). (*F* and *G*) Darkfield illumination after immunohistochemical detection of PHAL. (*H*) Photomicrograph illustrating dual immunofluorescence for CGRP and PHAL. In this experiment, the tracer was injected into the AIv, and axons were observed in a region encompassing the CbN and Parvafox nucleus. The borders of the PSTN/CbN are highlighted by CGRP innervation. (Scale bar, 500 μm.) cpd: cerebral peduncle; fx: fornix; mtt: mammillothalamic tract; ORB: orbital area; PH: posterior hypothalamic nucleus; PIR: piriform area; PMv: ventral premammillary nucleus; PVp: periventricular nucleus, posterior part; TMd: tuberomammillary nucleus, dorsal part.

described the structural organization of this network, which is strikingly reminiscent of the canonical hyperdirect and indirect pathways. Finally, we also illustrated functional PSTN-dependent electrophysiological and behavioral responses related to pain, sickness, and the inhibition of ingestive behavior conceptually homologous to the motor no-go response mediated by the STN-dependent indirect pathway.

Results

The Rat PSTN Complex and Network. The PSTN is the most conspicuous nucleus in the premammillary lateral hypothalamus. Laterally adjacent to the STN (*SI Appendix*, Fig. S1), it is also ventrally and medially neighbored by smaller cell groups, including the oval-shaped calbindin nucleus (CbN) described in the rat (12). Both the PSTN and CbN form a nuclear complex as they share several neurochemical and hodological features, including dense calcitonin-gene-related peptide (CGRP) innervation reportedly arising in the lateral parabrachial nucleus (PB) (*SI Appendix*, Fig. S1) and intense connections with the CEA (12, 16).

Both retrograde and anterograde tract-tracing approaches were employed to analyze the organization of projections from the INS to the PSTN/CbN. Retrograde tracer (fluorogold [FG]) injections centered in the PSTN resulted in the staining of cells distributed throughout the anteroposterior INS with the agranular insular dorsal (AId) and posterior (AIp) areas being intensely labeled. Dorsal and ventral to these areas, gustatory (GU), visceral (VISC), and agranular ventral (AIv) areas contained fainter and less abundant cell bodies (Fig. 1 *B* and *C*). The anterograde tracer *Phaseolus vulgaris* leucoagglutinin (PHAL) was then iontophoretically injected into the GU ($n = 2$), VISC ($n = 1$), AId ($n = 3$), AIv ($n = 1$), and AIp ($n = 1$) (Fig. 1*D* and *SI Appendix*, Fig. S2). Control injections were made in the motor (MO) ($n = 2$), somatosensory (SS) ($n = 2$), and orbital ($n = 2$) areas. The projections from the MO and SS to the STN illustrated the well-described basal ganglia hyperdirect pathway (Fig. 1 *E* and *F*). After PHAL injections in the INS, rather than targeting the STN, PHAL axons topographically innervated the adjacent PSTN/CbN (Fig. 1 *G* and *H*). The densest projections originated from injection sites in the AIp and AId, confirming the retrograde observation. However, each injection site in the INS provided a distinct pattern of distribution of PHAL axons within the PSTN/CbN complex. To better assess these different patterns of innervation, the distribution of the PHAL axons was compared with that of the immunofluorescent signals for calbindin, parvalbumin, and CGRP that were described in the rat PSTN/CbN (*SI Appendix*, Fig. S3) (12). After AIp injection, PHAL axons were codistributed with CGRP labeling in both the PSTN and CbN. In contrast, axons from injection sites in the AId, GU, and VISC innervated more dorsal regions of the PSTN and minimally involved the CbN (*SI Appendix*, Fig. S3). The AIv mostly innervated the CbN and the adjacent Parvafox nucleus. These results, consistent with the report by Babalian et al. (17) that the orbital cortices innervated the Parvafox nucleus (also

confirmed in our control experiments but not illustrated here), indicate that the frontal pole of the cerebral cortex, including the INS, innervates a large premammillary region of the lateral hypothalamus encompassing the STN, the PSTN/CbN complex, and the Parvafox nucleus in the rat in a topographically organized way (Fig. 1*E*).

The analysis of the distribution of PHAL axons from INS injection sites also suggested indirect anatomical links with the PSTN/CbN. Indeed, most INS PHAL injection sites also provided intense innervation of the CEA, known to have strong anatomical links with the PSTN/CbN complex (12). These projections, however, seemed to be best understood if interpreted within a more general context of corticostriatal projections (Fig. 2*A*). The topographic organization of cortical projections into the striatal compartment is an acknowledged anatomical fact. Whereas the MO and SS cortices innervated specific lateral and dorsal sectors of the caudoputamen nucleus (CPU), the INS provided an intense innervation of ventral components of the CPU, including the amygdalostriatal transition area (ASt), and of the ventral striatum (STRv), including the nucleus accumbens (ACB) (Fig. 3). From the AIv and AIp, the ventral striatal innervation fields also encompassed the olfactory tubercle (Fig. 2*A*). From most INS injection sites, the innervation of the ASt extended into the CEA. This was evident for GU and VISC projections that innervated the capsular part of the CEA (CEAc) (Figs. 2 *B* and *C* and 3 and *SI Appendix*, Figs. S4 and S5). These inputs were exclusively provided by axons exiting the ASt. From the anterior part of the GU, CEA innervation included the lateral domain of the lateral part (CEAl) (*SI Appendix*, Fig. S4). Finally, the CEAl as a whole was abundantly innervated by the caudal AId and the AIp (*SI Appendix*, Fig. S4). The medial part of the CEA (CEAm) was only discretely innervated by the rostral pole of the AId and the AIp. Therefore, based on the analysis of the distribution and pathways followed by PHAL axons, the striatal projection from the INS encompasses the capsular and lateral parts of the CEA.

The CEA is bidirectionally connected with the PSTN through its medial division, while the CEAc and CEAl send sparse inputs to this nucleus (16, 18, 19). To determine whether CEAc and CEAl could indirectly target the PSTN, we combined PHAL injections in the lateral CGRP-rich regions of the CEA with FG injections in the PSTN (Fig. 2 *D*–*F*). The distribution of PHAL axons matched that of the FG cells in the CEAm. However, we observed that the caudal substantia innominata (SI) contained denser innervation by PHAL axons as well as abundant FG-labeled cells. Apotome-assisted optical slicing and three-dimensional (3D) reconstructions identified many boutons in close contact with FG-containing cells, showing that lateral CEA regions target cells that innervate the PSTN, and these cells were observed in the caudal SI adjacent to the globus pallidus (GP) and to a lesser extent in the CEAm (Fig. 2*F*).

Therefore, the anatomy points to topological homologies between the networks involving the PSTN/CbN or the STN with hyperdirect-like projections from the INS that parallel the isocortical hyperdirect pathway to the STN and indirect inputs through the lateral CEA and caudal SI adjacent to the GP. In vivo electrophysiological recordings in both the STN and PSTN were also performed, demonstrating physiological similarities (*SI Appendix*). In fact, PSTN neurons had significantly lower spontaneous firing, but both the STN and PSTN exhibited the same pattern of activity, and neurons in both structures also similarly responded to a peripheral noxious stimulus (footshock) (*SI Appendix*).

C-Fos Expression in the Rat PSTN/CbN Complex in Relation to Neophobia or Sickness. We further sought to better functionally characterize the PSTN. To date, the only available information included c-Fos responses related to palatable food ingestion and satiety (12–15) as well as compulsive and anxious responses (20, 21). Owing to its intense CGRP inputs from the parabrachial neurons that also innervate the CEAc and CEAl, we hypothesized that the PSTN could be involved in sickness-induced anorexia, in line with the well-established role of CGRP projections from the same source into the lateral CEA (22, 23). In addition, the INS and CEA are involved in neophobia-induced prevention of feeding (24–26). Therefore, we evaluated the influence of the PSTN/CbN in experiments where feeding is prevented by neophobia or by administration of the bacterial endotoxin lipopolysaccharide (LPS) or the anticancer chemotherapy drug cisplatin.

First, we performed a neophobic experiment with 20% sucrose. Neophobic experiments are often performed with saccharin. However, saccharin does not induce intense c-Fos expression in the PSTN, and we previously demonstrated that the PSTN does not react to an increase in glycemia induced by intraperitoneal (i.p.) glucose injections (12). The licking profile of rats habituated to drinking the sucrose solution was markedly different from that of neophobic rats that tasted this solution for the first time (Fig. 4*A*). Neophobic rats also consumed significantly less of the solution than control habituated rats (Fig. 4*B*). Nuclei labeled by the c-Fos antibody were significantly more abundant in the PSTN in neophobic rats compared to controls. No significant difference was observed in the CbN (Fig. 4*C*). The anatomical localization of c-Fos nuclei was confirmed by colabeling with the anti-CGRP antibody (Fig. 4 *D* and *E*).

Second, sickness was caused by i.p. injection of LPS (5 mg/kg) or cisplatin (6 mg/kg). Very intense expression of c-Fos was observed in the CGRP neurons of the lateral PB, as previously described in the literature (22, 23) (*SI Appendix*, Fig. S6). Overall, the LPS-induced responses were higher than those obtained after cisplatin injections. Both conditions triggered an increase in c-Fos expression in both the PSTN and CbN (Fig. 4*F*). However, the response appeared more intense in the CbN. Because the CbN is rich in calbindin-containing neurons, double labeling c-Fos/calbindin showed that few of the c-Fos nuclei belonged to calbindin cells. Attempts to identify the neurochemical nature of the remaining cells were not successful.

Genetic Tracing and Pharmacogenetic Manipulation in the Mouse. The data described above suggested that the PSTN/CbN complex is involved in the modulation of consummatory behavior depending on cognitive (novelty) and interoceptive (sickness, inflammatory) signals. To confirm and extend this observation, we further manipulated the PSTN using pharmacogenetic tools in mice. However, the PSTN in this species has not been investigated to date, although the nucleus has been identified in mouse brain atlases (27, 28). The mouse CbN has not yet been identified. Therefore, we conducted a pilot study to verify that the mouse and rat PSTN/CbN are comparable. The combination of results from immunohistochemistry or using viral tract tracing in mice with resources from the Allen Brain Institute database (28) provided convincing evidence that the PSTN/CbN in mice shares many features of the rat complex, but important differences were also identified, mostly about the neurochemical nature of the CbN. One of the main differences was the absence of intense calbindin expression in the mouse CbN (*SI Appendix*, Fig. S7). Using immunohistochemistry and confirmed by the in situ hybridization method in the Allen Brain Atlas (28), only a few calbindin cells are observed in the region. In contrast, the *tac1* gene is very intensely expressed in both the PSTN and CbN, as illustrated in the Allen Brain Atlas (*SI Appendix*, Fig. S7). However, as in the rat, immunohistochemistry was not efficient in labeling substance P perikarya in the nucleus, and the use of colchicine was not suitable for our experiments. We turned to the use of a Tac1-cre mouse line to pursue our investigations.

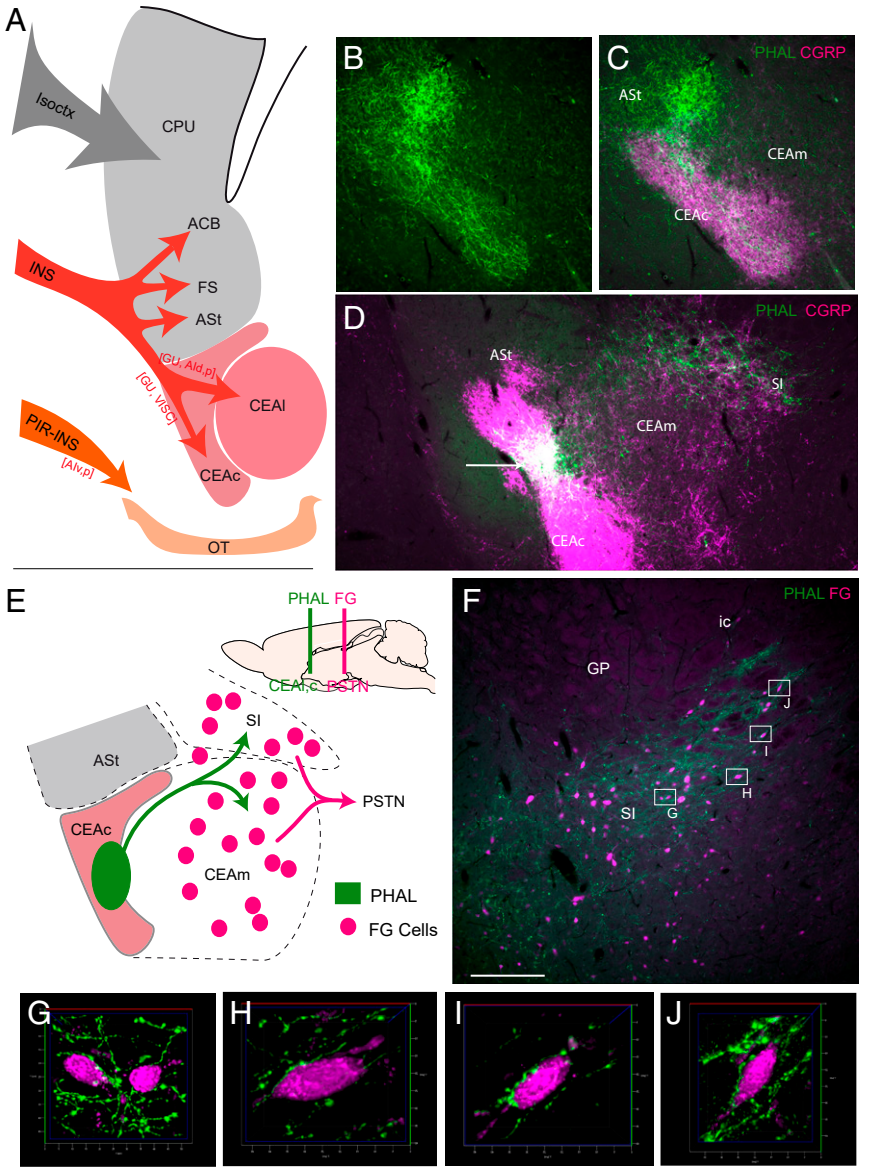

Fig. 2. The insular cortex-ventral striatum/CEA-PSTN network maps onto a basal ganglia-like indirect pathway organization. (*A*) Line drawing illustrating the topographic organization of projections from the cortex to the STR with the isocortex innervating the caudoputamen (CPU or dorsal striatum) while the INS as a whole targets the CPU and ventral striatum, including the ASt, ACB, FS, and OT. From the ASt, the INS also innervates the CEAc and CEAl. (*B* and *C*) Dual immunofluorescence to detect PHAL and CGRP. After PHAL injection in the GU, intense labeling of the ASt is observed, but axons exit this region to further reach the CEAc that is characterized by dense CGRP positive inputs from the PB. (*D*) Photomicrograph showing a PHAL injection site in the CGRP-rich CEAc. PHAL axons leave the CEAc and enter the CEAm but provide a denser input to the caudal SI. (*E*) Line drawing illustrating the indirect pathway from the CEAc to the PSTN as observed after PHAL injection in the CEAc and FG injection in the PSTN. (*F*) Dual immunofluorescence photomicrograph of a section through the caudal SI. This region contains abundant FG-labeled cells in close apposition with PHAL axons after injections of FG in the PSTN and PHAL in the CEAc. (*G–J*) Apotome-assisted optical slicing and 3D reconstructions of neurons identified in *F* show many boutons in close contact with FG-containing cells. (Scale bar, 250 μm in *B–D* and 500 μm in *F*.) ASt: amygdalostriatal transition area; ACB: accumbens nucleus; AId: agranular insular dorsal area; AIp: agranular insular posterior area; AIv: agranular insular ventral area; CEAc: central nucleus amygdala, capsular part; CEAl: central nucleus amygdala, lateral part; CEAm: central nucleus amygdala, medial part; cpd: cerebral peduncle; CPU: caudoputamen nucleus; FS: fundus striatum; ic: internal capsule; INS: insular area; Isoctx: isocortex; GP: globus pallidus; GU: gustatory area; PIR: piriform area; OT: olfactory turbercle; SI: substantia innominata; VISC: visceral area.

The iontophoretic injection of a Cre-dependent adeno-associated virus (AAV-pCAG-FLEX-EGFP-WPRE) in Tac1-cre mice resulted in the very intense labeling of a dense group of cells in both the PSTN and CbN with only scattered labeled neurons in adjacent tissues (Fig. 5 *A* and *B*). Labeled axons from the infection site were traced rostrally in the telencephalon where they provided an intense innervation of the caudal SI adjacent to the GP and of the CEAm, but not of the CEAl,c identified by CGRP immunostaining (Fig. 5 *D–F*). Other projections involved the INS, bed nuclei of the stria terminalis (BST), and paraventricular thalamic nucleus (PVT), and caudally, the PB and nucleus of solitary tract (NTS) (Fig. 5*C*). The overall Tac1-cre neuron projections are therefore very similar to those described by the PHAL method for the whole nucleus in the rat (11, 12).

Recombinant transsynaptic pseudorabies virus (PRV)152 and PRV2001 stereotaxic injections were also made in the CEA of Tac1-cre mice and resulted, after a short survival time, in the

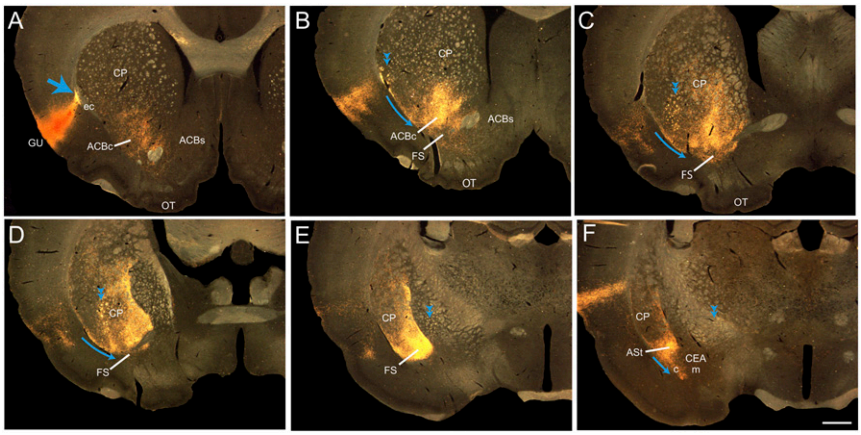

Fig. 3. Pathway from the INS into the striatum. (*A–F*) Photomicrographs illustrating the course of PHAL axons in the striatal compartment after PHAL injection in the GU. PHAL axons enter the external capsule (large blue arrow in *A*), some join the internal capsule (double arrowheads) and travel through the striatum and the pallidum to reach the diencephalon, while others (blue arrows) take a ventral route to enter the striatal compartment. The innervation of the CEAc arises from axons extending from the FS or from the ASt and, therefore, is an extension of the striatal pathway. (Scale bar, 1 mm.) ASt: amygdalostriatal transition area; ACBc: accumbens nucleus, capsule; ACBs: accumbens nucleus, shell; CEAc: central nucleus amygdala, capsular part; CEAm: central nucleus amygdala, medial part; CPU: caudoputamen nucleus; ec: external capsule; FS: fundus striatum; ic: internal capsule; INS: insular area; Isoctx: isocortex; GP: globus pallidus; GU: gustatory area; PIR: piriform area; OT: olfactory turbercle.

intense retrograde labeling of cells restricted to the PSTN/CbN, confirming that the origin of the projections to the CEA from this lateral hypothalamus (LHA) region is restricted to the PSTN/CbN, as it is in the rat (12) (*SI Appendix*, Fig. S8). PRV2001 is cre-specific; it labels Tac1 neurons in the PSTN, confirming that these neurons project into the CEA. The

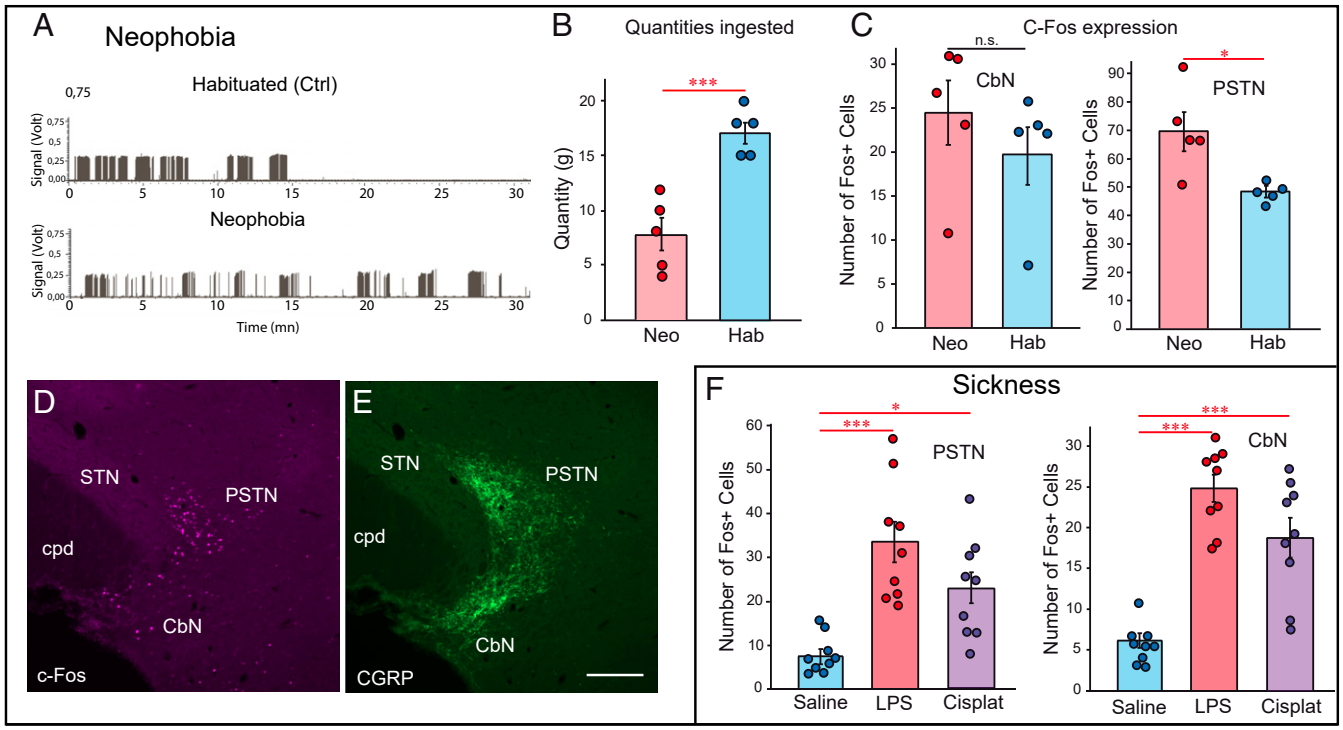

Fig. 4. C-Fos expression in the rat PSTN/CbN. (*A*) Examples of licking profiles for habituated (control) and neophobic rats. Habituated rats rapidly drank a large amount of the solution, while the neophobic rats spread their consumption of the same solution over the entire 30-min period. (*B*) Graphs illustrating that habituated (controls) rats consumed significantly more of the 20% sucrose solution than the neophobic rats ($n = 5$ in each group, unpaired t test, $P = 0.0008$, $^{***}P < 0.001$). (*C*) Neophobic rats display a higher number of c-Fos-expressing nuclei in the PSTN than habituated control rats that already encountered the sucrose (20% vol/vol) solution ($n = 5$ rats; unpaired t test, $P = 0.0181$). The increase in the number of c-Fos nuclei in the CbN was not significant ($n = 5$ rats; unpaired t test, $P = 0.3526$). (*D* and *E*) Photomicrographs illustrating c-Fos expression in the PSTN of neophobic rats (*D*). The same section was labeled with an anti-CGRP antibody to identify the borders of the PSTN/CbN (*E*). (*F*) Sickness induced by either an i.p. injection of LPS or cisplatin induced a very significant increase in c-Fos expression in both the PSTN and CbN ($n = 9$ rats; one-way ANOVA and Bonferroni's post hoc multiple comparison test; for the PSTN, $F = 13.91$, and for the CbN, $F = 29.67$). (Scale bar, 200 μm.) $^{*}P < 0.05$; $^{***}P < 0.0001$; n.s. = not significant. CbN: calbindin nucleus; cpd: cerebral peduncle; PSTN: parasubthalamic nucleus; STN: subthalamic nucleus.

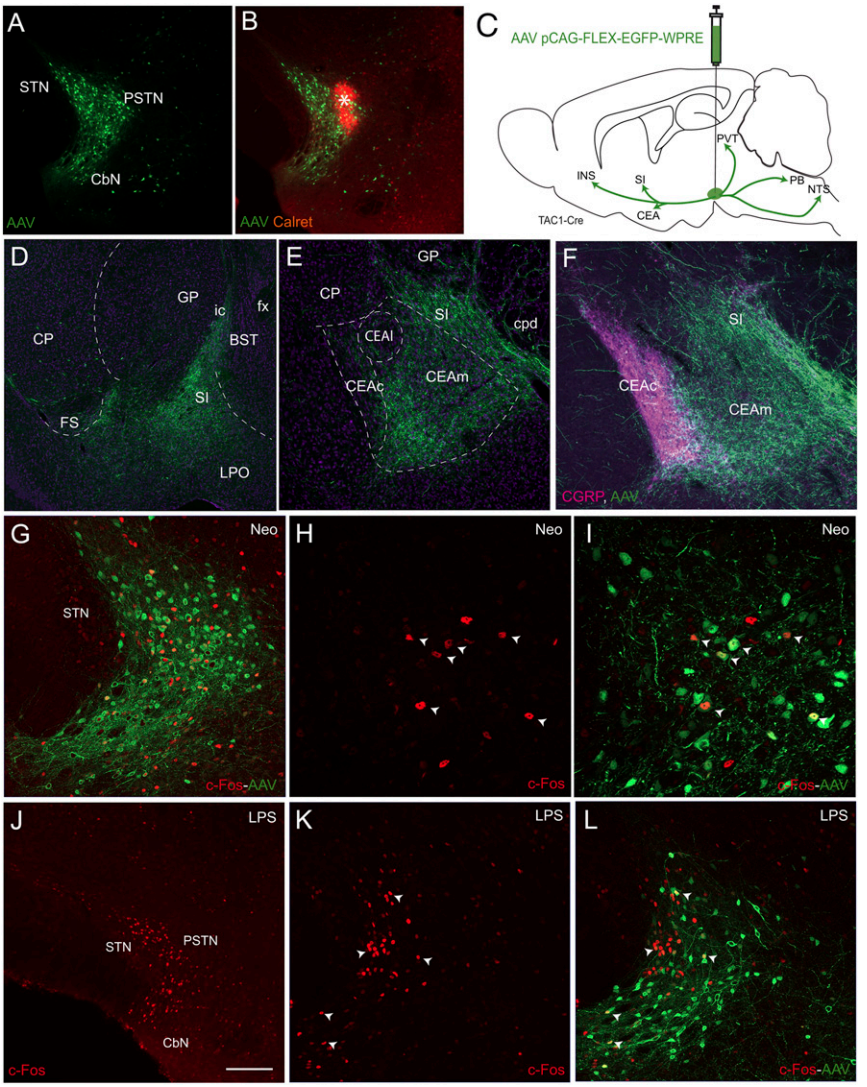

Fig. 5. Anatomical characterization of the mouse PSTN. AAV pCAG-FLEX-EGFP-WPRE injections in the PSTN allowed us to identify the projections of the nucleus in a Tac1-cre mouse line. (*A* and *B*) Injection site of the AAV (*A*) labeled a dense condensation of cells in the PSTN that extended into the CbN. The same section labeled with an anti-calretinin antibody (*B*) allowed us to see the center of the injection (*). (*C*) Line drawing that summarizes the projections labeled by the virus. As in the rat, projections were observed in the CEAm, posterior SI, and BST. Dorsally, the projections reach the caudal PVT. Caudally, the projections are traced to the parabrachial nucleus and the nucleus of the solitary tract. Overall, the projections of the $PSTN^{Tac1}$ cells are very similar to those described for the PSTN in the rat. (*D–F*) Photomicrographs to illustrate the distribution of axons in the caudal SI (*D*) and in the CEAm (*E* and *F*). In *F*, dual fluorescence (AAV and immunofluorescence for CGRP) illustrates the innervation of the CEAm and caudal SI by anterogradely labeled $PSTN^{Tac1}$ axons, while the CEAc that contains intense CGRP innervation is not targeted. Sections *D* and *E* are counterstained with a nuclear marker (NeuroTrace 640/660 deep-red fluorescent Nissl stain). (*G–I*) Photomicrographs of a section after injection of the AAV pCAG-FLEX-EGFP-WPRE in the PSTN of a Tac1-cre mouse. The mouse was subjected to neophobia by exposure to a novel sucrose solution before perfusion. This condition induced high c-Fos expression in the PSTN. A large proportion of the c-Fos-labeled nuclei belong to Tac1-cre cells. Arrowheads in *H* and *I* point to double-labeled cells at higher magnification. (*J–L*) Injection of LPS in a mouse 3 h before killing induced very high expression of c-Fos in both the PSTN and CbN (*J*). After injection of the AAV pCAG-FLEX-EGFP-WPRE, many c-Fos nuclei belong to Tac1-cre neurons in both nuclei (arrowheads in *K* and *L*). (Scale bar, 200 μm in *A*, *E*, and *J*; 100 μm in *F*, *G*, *K*, and *L*; and 50 μm in *H* and *I*.) ACB: accumbens nucleus: BST: bed nuclei of the stria terminalis; CbN: calbindin nucleus; CEAc: central nucleus amygdala, capsular part; CEAl: central nucleus amygdala, lateral part; CEAm: central nucleus amygdala, medial part; cpd: cerebral peduncle; CP: caudoputamen nucleus; FS: fundus striatum; ic: internal capsule; INS: insular area; GP: globus pallidus; GU: gustatory area; LPO: lateral preoptic area; PIR: piriform area; PVT: paraventricular nucleus thalamus; OT: olfactory turbercle; SI: substantia innominata.

retrograde tracer cholera toxin (subunit b) was also injected in the PSTN and resulted in retrogradely labeled cells with a pattern that was similar to that described in the rat. This pattern included cells labeled in the INS, caudal SI, and CEAm (*SI Appendix*, Fig. S8). Dual injections of PHAL in the INS and of the AAV-pCAG-FLEX-EGFP-WPRE in the PSTN/CbN allowed us to verify that PHAL axons from the INS make boutons on GFP cells in the PSTN (*SI Appendix*, Fig. S8). Finally, images from the Allen Brain Atlas showed that anterograde genetic tract tracing from the INS, caudal SI, and CEA confirmed the very intense and specific nature of the projections from these structures to the PSTN/CbN (*SI Appendix*, Fig. S9), similar to what was reported in the rat in this study as well as others (11, 12, 16, 19, 29–31). Hence, the overall anatomy of the mouse PSTN/CbN is similar to that of the rat PSTN/CbN. To verify that these nuclei express c-Fos under similar conditions, mice received an iontophoretic injection of AAV-pCAG-FLEX-EGFP-WPRE in the PSTN/CbN. Ten days later, some of them ($n = 3$) were deprived

of drinking solution for 12 h (overnight) and then given access to a 10% sucrose solution for 30 min before being perfused with the fixative solution. This experiment resulted in an intense expression of c-Fos in fluorescent Tac1 cells in the PSTN; however, not all c-Fos nuclei belonged to Tac1 cells (Fig. 5 *G–I*). In another group of mice ($n = 6$), a single injection of LPS (50 μg/kg) was administered 3 h before killing. Again, intense expression of c-Fos was observed in the PSTN/CbN complex, and many labeled nuclei belonged to fluorescent Tac1-cre neurons (Fig. 5 *J–L*). The numbers of double-labeled neurons were not counted as they would vary with the position of the AAV injection site. Therefore, the mouse PSTN/CbN complex and within it the Tac1-cre cells appear to be involved in similar functional responses to the rat PSTN/CbN with regard to c-Fos expression.

To interfere with PSTN-dependent function, DREADD experiments were conducted with the pAAV-hSyn-DIO-hM4D(Gi)-mCherry recombinant viral vector bilaterally injected into the PSTN of Tac1-cre mice (Fig. 6*A*). Remarkably, whereas clozapine-N-oxide (CNO) injection had no effect on spontaneous food intake, locomotion (open field test), or affective/coping behavior (forced swim test) (Fig. 6 *B–D*), it did suppress the neophobic response, thereby reinstating consummatory behavior (Fig. 6*E*).

In the last experiment, we tested whether feeding/drinking behavior could be reinstated in sick animals by manipulating the PSTN circuitry. To prevent confounding by neophobia, pAAV-hSyn-DIO-hM4D(Gi)-mCherry–injected Tac1-cre mice were first habituated for 1 wk to drink a sucrose (10% vol/vol) solution before being deprived for 12 h. Mice then received i.p. injections of LPS (50 μg/kg) and CNO (1 mg/kg; two injections) and, 3 h after LPS injection, placed in operant chambers equipped with lickometers to monitor sucrose (10% vol/vol) solution consumption. As expected, control mice refrained from drinking. In contrast, accurate chemogenetic inactivation of the PSTN relieved this inhibition, and experimental mice consumed (more), performing a significantly higher number of licks than the control and mistargeted (AAV injections in the zona incerta, ventral tegmental area [VTA] or supramammillary nucleus) mice (Fig. 6*F*).

Discussion

The Organization of the PSTN Complex Network. The overall anatomical data obtained in this study point to the conclusion that the INS-CEA/caudal SI-PSTN/CbN structures are involved in a complex network and that the general structural organization of this network is reminiscent of that of the canonical hyperdirect and indirect pathways from the motor cortex that involve the striatum, pallidum, and STN. This comparison is primarily based on the topographic organization of the direct and indirect projections from the INS to the PSTN, which run parallel to the basal ganglia pathways, with INS adjacent to the MO/SS projecting to the CEAc,l adjacent to the striatum and to the PSTN adjacent to the STN (Fig. 6*G*). Finally, CEAc,l innervates the caudal SI adjacent to the GP, which in turn innervates the PSTN/CbN, in a similar manner as the GP innervates the STN. This assumption supposes that CEAc,l belongs to the striatum. This was proposed as early as the work of Gurdjian (32) and Brodal (33) and then confirmed by McDonald (34), who described medium spiny neurons in these two cell groups identical to the medium spiny neurons of the caudoputamen nucleus; this was again extensively discussed by Petrovich and Swanson from neurochemical and hodological levels (8, 35) and, finally, also implied by developmental approaches (9). Recently, Kim et al. (36) showed that the CEA expresses indirect pathway markers and described basolateral amygdala projections to the CEA with neurochemical characteristics of corticostriatal connections. Alheid (37) also admitted that the concept of the extended amygdala could be adapted to a simplified structural plan of the forebrain in which the lateral CEA can be compared to the striatum and the medial CEA as well as the caudal SI associated with the pallidum [figure 3 in Alheid (37)]. Following the same line of thinking, the PSTN/CbN and the STN are somehow related. Altmann and Bayer were the first to associate the STN to the hypothalamus when they described a common developmental origin for this nucleus and the premammillary region of the hypothalamus to which the PSTN and CbN belong (38). This was then confirmed, as the STN and the premammillary region share a similar early molecular signature in the embryo (39–42). In adult animals, both the STN and PSTN/CbN express Vglut2 and are glutamatergic, while they do not contain GABA (12, 43, 44). Moreover, Groenewegen and Berendse had already highlighted the resemblance with both the STN and the neighboring LHA neurons corresponding to the PSTN (45). Finally, we also provided evidence that the electrophysiological profiles of neurons in both the STN and PSTN are similar. It is worth mentioning here that, in primates including human, the hyperdirect pathway from the prefrontal and insular cortices admittedly encompasses the region of the LHA medially adjacent to the STN that may correspond to the PSTN (46, 47). In humans, the LHA adjacent to the STN is calbindin and calretinin positive, which is one of the neurochemical characteristics of the PSTN/CbN complex in rats (48).

If the general structure of the INS-PSTN/CbN network shows a similar organization to that of the cortical/basal ganglia hyperdirect/indirect pathways, the detailed analysis of this network has revealed an extraordinarily complex design. The hyperdirect component of this network involves either the PSTN, the CbN, or both. The PSTN itself is not homogeneous. Its cyto- and chemoarchitecture have not yet been fully described, but it is clear that several cell types compose this nucleus as well as the CbN. AIp or AId/GU/VISC innervates lateral and dorsomedial sectors differently within the PSTN, along the CGRP inputs from the PB. It is to be remembered here that the isocortex also topographically innervates the STN. Therefore, the organization of the hyperdirect pathway from the cerebral cortex topographically innervates the STN, PSTN, CbN, and perhaps also the Parvafox nucleus.

The indirect part of this network is even more complex. The CEAc receives convergent inputs from the GU and VISC, the lateral aspect of the CEAl receives convergent inputs from the GU and AID/AIp, while the medial aspect of the CEAl receives projections from the AId and AIp. This topographic pattern of innervation of the CEAc,l is reminiscent of the cortical projections that innervate distinct band-shaped domains within the caudoputamen nucleus, but each of these domains receives convergent inputs from several distinct cortical areas. This arrangement in the structural organization of connections between the cortex and striatum was interpreted by Graybiel as important for learning and may play a role in habit acquisition (49–52). From a single injection site in the INS, striatal projections involved parts of the caudoputamen and ventral striatum, including the nucleus accumbens and olfactory tubercle, each at the origin of distinct branches of the basal ganglia network, therefore implying the multiple processes related to motor, motivation, and cognitive responses initiated from the INS. However, it is compelling that the hyperdirect pathway from the INS targets the PSTN/CbN rather than the STN, which strongly suggests the importance of this hypothalamic complex in the global INS network.

The PSTN/CbN Gates Feeding Behavior. More effort will be necessary to fully unravel the overwhelmingly complex anatomical organization of the INS-PSTN/CbN network. In this context, our contribution to the understanding of its function illustrates that it processes cognitive as well as interoceptive signals to gate

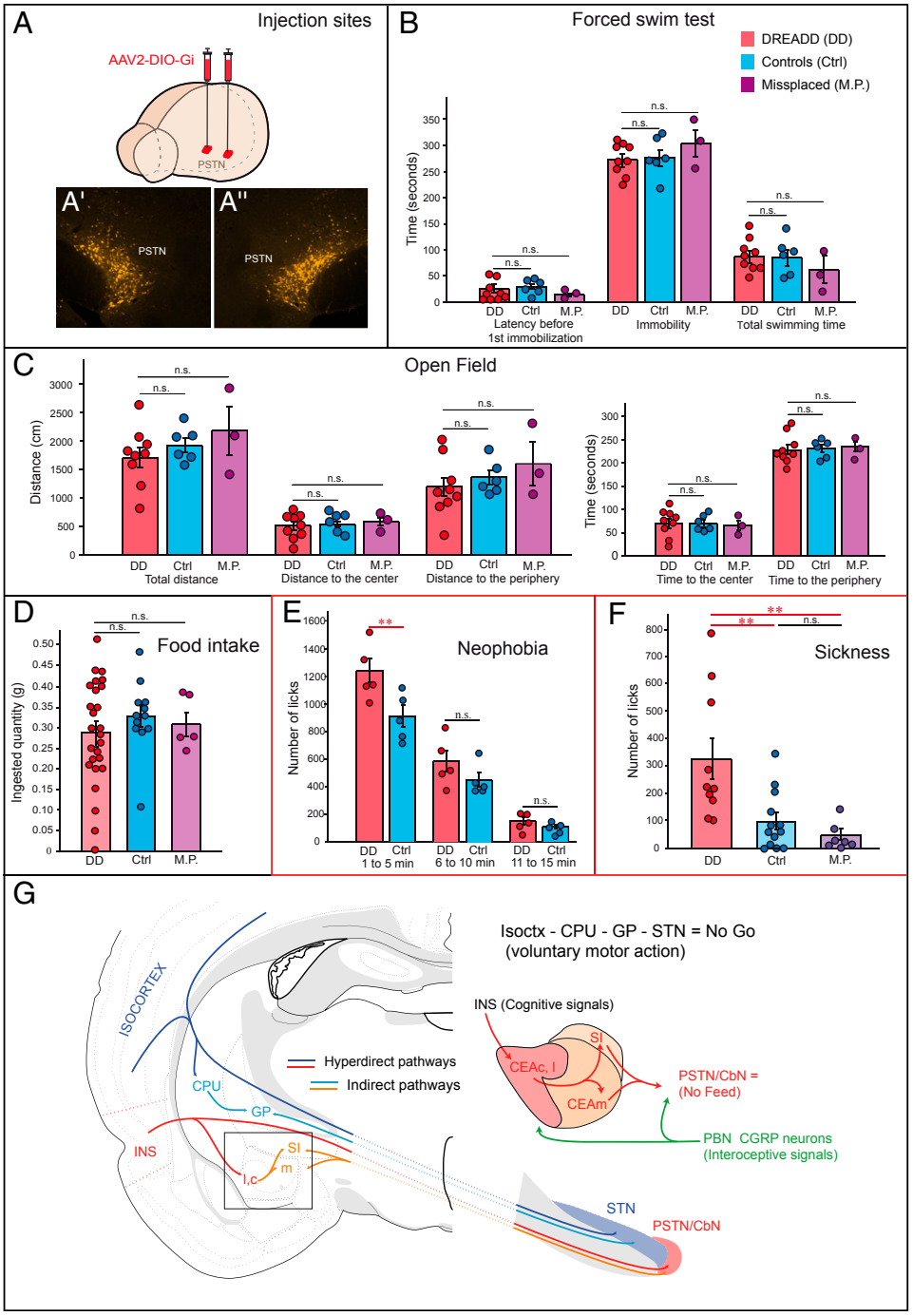

Fig. 6. DREADD experiments and concluding diagram. (*A*) Diagram shows pAAV-hSyn-DIO-hM4D(Gi)-mCherry bilateral injections in the PSTN of Tac1-cre mice. (*A′* and *A′′*) illustrate injection sites of the virus in the PSTN/CbN. (*B*) No difference in the forced swim test was obtained after CNO injection. Several parameters were analyzed: latency before first immobilization, duration of immobilization, and total swimming time. Controls, $n = 6$; DREADD, $n = 9$; DREADD misplaced (M.P.), $n = 3$; two-way ANOVA and Bonferroni's multiple comparison test, $P = 0.9146$, $F = 0.09$. (*C*) Open field test performance was also not affected by DREADD inhibition of Tac1 neurons. Controls, $n = 6$; DREADD, $n = 9$; DREADD M.P., $n = 3$; two-way ANOVA and Bonferroni's multiple comparison test: for "time," $P = 1$, $F = 0$; for "distance," $P = 0.1350$, $F = 2.09$. (*D*) CNO in Tac1-cre mice injected with pAAV-hSyn-DIO-hM4D(Gi)-mCherry did not significantly affect food ingestion. Controls, $n = 12$; DREADD, $n = 18$; DREADD M.P., $n = 5$; one-way ANOVA and Bonferroni's multiple comparison test, $P = 0.6135$, $F = 0.4947$. (*E*) Chemogenetic inhibition of PSTN (Tac1 neurons) suppresses neophobia, with mice initiating more consummatory behaviors (number of licks) toward the never-encountered solution (10% sucrose) during the first period of the trial (minutes 1 to 5) compared to control (Ctrl) mice ($n = 5$ mice; two-way ANOVA and Bonferroni's multiple comparison test, $P = 0.026$, $F = 11.25$). (*F*) Similarly, CNO inhibition of the PSTN reinstates consummatory behavior suppressed by LPS-induced sickness, with CNO-administered PSTN mice displaying more licks than control mice and CNO mice with M.P. AAV injections (ctrl, $n = 13$; DREADD, $n = 10$; DREADD M.P., $n = 7$; one-way ANOVA and Bonferroni's multiple comparison test, $P = 0.0015$, $F = 8.377$). The diagram in *G* highlights the homology of the hyperdirect and indirect pathways involving, on the one hand, the isocortex-CPU-STN network and, on the other hand, the INS-CEA-PSTN/CbN circuit with a focus on cognitive and interoceptive inputs influencing the latter circuit. $^{**}P < 0.001$; n.s. = not significant. CbN: calbindin nucleus; CEAc: central nucleus amygdala, capsular part; CEAl: central nucleus amygdala, lateral part; CEAm: central nucleus amygdala, medial part; CPU: caudoputamen nucleus; INS: insular area; GP: globus pallidus; GU: gustatory area; SI: substantia innominata; PSTN: parasubthalamic area.

ingestive behavior. Exposure to a palatable tastant induced a high expression of c-Fos in the PSTN (12), and this expression was even higher if the tastant was unknown to the animal when the ingested volume was low. Therefore, the nucleus does not react to the quantity or volume of ingested food, but rather c-Fos expression was associated with cognitive information presumably related to the hedonic quality of the aliment and its novelty. DREADD inhibition of PSTN Tac1-cre neurons in mice decreased the neophobic response. As the novel characteristics of a food source is determined in the telencephalon and includes interactions between structures such as the INS, the hippocampal formation, and the amygdala, this information is presumably provided to the PSTN by descending projections, perhaps from the INS. However, it cannot be ruled out that the PSTN reacts to anxiety signals from the CEA. Substance P, which is coded by the *tac1* gene, and the receptor NK-1 are implicated in a variety of processes, including stress regulation and anxiety-related behavior (53). The CEA is one of the brain sites in which SP may exert its action on anxiety and this nucleus is critical for control of feeding by aversive learned cues (54, 55). The PSTN could be one source of SP to the CEA. DREADD inhibition of PSTN-Tac1 neurons did not produce any significant response in the forced swim test, although this does not preclude that activation of these neurons may have ended in different results. Interestingly, CGRP neurons in the PB that abundantly innervate the PSTN/CbN have been reported to sense danger and also be involved in neophobia (56, 57). The PB^{CGRP} neurons, which also express SP as well as neurotensin (58), and the PSTN/CbN are part of the same network as the CEA and INS and therefore are involved in similar responses.

However, PB^{CGRP} neurons have been mostly described as relaying pain, inflammation, and visceral discomfort signals from the periphery (56). Again, the PSTN/CbN reacted to similar stimuli. The CbN appeared to respond at least as intensely as the PSTN, which was not the case for neophobia. Notably, c-Fos is highly expressed in both rat and mouse PSTN/CbN without any food ingestion after LPS injection, which suggests that these cell groups may be involved in functions unrelated to ingestive behavior but these functions need to be identified. Nevertheless, sickness conditions are known to produce an anorexic response, and DREADD inhibition of the Tac1-cre neurons in the PSTN/CbN at least partly reversed this response. Again, a similar result was obtained after inhibition of the PB^{CGRP} neurons, and this effect was mediated by the CEAc (22). In our study, we left the PB^{CGRP} to the CEAc pathway untouched, as the PSTN is connected to the CEAm and caudal SI. Therefore, we impacted the network downstream from the CEAc, indicating either that damaging the network at any level diminishes the anorexic response associated with sickness or that an intact PSTN/CbN is necessary to relay the CEA information processing and anxiety-related signals to downstream centers (59, 60) or back to the telencephalon through the thalamus (61, 62).

Conclusions

Inhibition of the PSTN/CbN suppresses the anorexic response associated with neophobia or sickness, indicating that the PSTN modulates the ingestion of palatable food. Hence, the PSTN gates a stop signal or warning no-eat signal for survival purposes in conflicting situations of potentially noxious (sickness-associated or previously unknown) sources of food to refrain from or initiating feeding by integrating interoceptive and cognitive signals. In certain aspects, the gating of CEA-triggered feeding exerted by the PSTN can be compared to the role of the adjacent STN in movement inhibition preventing information flow from the striatum in a no-go pathway (Fig. 6*G*). Collectively, these results highlight the basal ganglia-like hyperdirect and indirect organization of the projections from the INS to the PSTN/CbN and emphasize the role of this complex, which exerts cognitive and interoceptive gating of feeding behavior.

Materials and Methods

All experiments presented in this study were conducted according to the animal research guidelines from the Directive 2010/63/EU of the European Parliament and of the Council of 22 September 2010 on the protection of animals used for scientific purposes. The protocols were approved by the Franche-Comté University's Animal Care Committee, and the investigators received authorization to conduct the study.

All rats and mice used in the experiments were housed under a 12 h/12 h light/dark cycle. The rats (Sprague–Dawley unless otherwise specified) were obtained from Janvier, and mice were obtained from The Jackson Laboratory. At the time of the experiments, Tac1-cre (B6;129S-Tac1tm1.1[cre]Hze/J) mice were 15 to 20 wk old and weighed ~25 to 28 g; Sprague–Dawley male rats were 10 to 15 wk old and weighed 300 to 320 g. All animals were used in scientific experiments for the first time. This includes no previous exposure to pharmacological substances or altered diets. Health status was normal for all animals. After surgery, rats and mice were allowed to recover for 7 to 15 d before further experiments. Antibodies, compounds, and the experimental procedures with the coordinates of all injection sites are described in *SI Appendix*.

Data Availability. All relevant data are within the manuscript and *SI Appendix*.

ACKNOWLEDGMENTS. This work was supported by the Region Franche-Comté, France. We are grateful to Prof. Lynn W. Enquist from Princeton University for kindly providing the PRV viruses used in this study.

1. R. Nieuwenhuys, The insular cortex: A review. *Prog. Brain Res.* **195**, 123–163 (2012).
2. C. Lu *et al.*, Insular cortex is critical for the perception, modulation, and chronification of pain. *Neurosci. Bull.* **32**, 191–201 (2016).
3. A. D. Craig, A rat is not a monkey is not a human: Comment on mogil (Nature Rev. Neurosci. 10, 283–294 [2009]). *Nat. Rev. Neurosci.* **10**, 466 (2009).
4. E. E. Benarroch, Physiology and pathophysiology of the autonomic nervous system. *Continuum (Minneap. Minn.)* **26**, 12–24 (2020).
5. R. L. Albin, A. B. Young, J. B. Penney, The functional anatomy of basal ganglia disorders. *Trends Neurosci.* **12**, 366–375 (1989).
6. C. R. Gerfen, J. P. Bolam, "The Neuroanatomical Organization of the Basal Ganglia" in *Handbook of Behavioral Neuroscience, Handbook of Basal Ganglia Structure and Function*, H. Steiner, K. Y. Tseng, Eds. (Elsevier, ed. 2, 2016), Vol. chap. 1, pp. 3–32.
7. A. Nambu, M. Takada, M. Inase, H. Tokuno, Dual somatotopical representations in the primate subthalamic nucleus: Evidence for ordered but reversed body-map transformations from the primary motor cortex and the supplementary motor area. *J. Neurosci.* **16**, 2671–2683 (1996).
8. L. W. Swanson, G. D. Petrovich, What is the amygdala? *Trends Neurosci.* **21**, 323–331 (1998).
9. M. Bupesh, A. Abellán, L. Medina, Genetic and experimental evidence supports the continuum of the central extended amygdala and a mutiple embryonic origin of its principal neurons. *J. Comp. Neurol.* **519**, 3507–3531 (2011).
10. P. Y. Wang, F. C. Zhang, *Outline and Atlas of Learning Rat Brain Slices*, (Westnorth University Press, 1995).
11. M. Goto, L. W. Swanson, Axonal projections from the parasubthalamic nucleus. *J. Comp. Neurol.* **469**, 581–607 (2004).
12. S. Chometton *et al.*, A premammillary lateral hypothalamic nuclear complex responds to hedonic but not aversive tastes in the male rat. *Brain Struct. Funct.* **221**, 2183–2208 (2016).
13. G. Zséli *et al.*, Elucidation of the anatomy of a satiety network: Focus on connectivity of the parabrachial nucleus in the adult rat. *J. Comp. Neurol.* **524**, 2803–2827 (2016).
14. G. Zséli *et al.*, Neuronal connections of the central amygdalar nucleus with refeeding-activated brain areas in rats. *Brain Struct. Funct.* **223**, 391–414 (2018).
15. A. M. Douglass *et al.*, Central amygdala circuits modulate food consumption through a positive-valence mechanism. *Nat. Neurosci.* **20**, 1384–1394 (2017).
16. M. Barbier, S. Chometton, Y. Peterschmitt, D. Fellmann, P.-Y. Risold, Parasubthalamic and calbindin nuclei in the posterior lateral hypothalamus are the major hypothalamic targets for projections from the central and anterior basomedial nuclei of the amygdala. *Brain Struct. Funct.* **222**, 2961–2991 (2017).
17. A. Babalian *et al.*, The orbitofrontal cortex projects to the parvafox nucleus of the ventrolateral hypothalamus and to its targets in the ventromedial periaqueductal grey matter. *Brain Struct. Funct.* **224**, 293–314 (2019).
18. T. S. Gray, M. E. Carney, D. J. Magnuson, Direct projections from the central amygdaloid nucleus to the hypothalamic paraventricular nucleus: Possible role in stress-induced adrenocorticotropin release. *Neuroendocrinology* **50**, 433–446 (1989).
19. G. D. Petrovich, L. W. Swanson, Projections from the lateral part of the central amygdalar nucleus to the postulated fear conditioning circuit. *Brain Res.* **763**, 247–254 (1997).

20. W. Han *et al*., Integrated control of predatory hunting by the central nucleus of the amygdala. *Cell* **168**, 311–324.e18 (2017).
21. Y. Ohmura *et al*., Different roles of distinct serotonergic pathways in anxiety-like behavior, antidepressant-like, and anti-impulsive effects. *Neuropharmacology* **167**, 107703 (2020).
22. M. E. Carter, M. E. Soden, L. S. Zweifel, R. D. Palmiter, Genetic identification of a neural circuit that suppresses appetite. *Nature* **503**, 111–114 (2013).
23. M. E. Carter, S. Han, R. D. Palmiter, Parabrachial calcitonin gene-related peptide neurons mediate conditioned taste aversion. *J. Neurosci.* **35**, 4582–4586 (2015).
24. J.-Y. Lin, J. Arthurs, S. Reilly, Gustatory insular cortex, aversive taste memory and taste neophobia. *Neurobiol. Learn. Mem.* **119**, 77–84 (2015).
25. J.-Y. Lin, S. Reilly, Amygdala-gustatory insular cortex connections and taste neophobia. *Behav. Brain Res.* **235**, 182–188 (2012).
26. A. Skórzewska *et al*., GABAergic control of the activity of the central nucleus of the amygdala in low- and high-anxiety rats. *Neuropharmacology* **99**, 566–576 (2015).
27. G. Paxinos, K. B. J. Franklin, *Paxinos and Franklin's the Mouse Brain in Stereotaxic Coordinates*, (Academic Press, ed. 5, 2019).
28. Allen Institute, Allen mouse brain atlas. https://mouse.brain-map.org/. Accessed 17 June 2020.
29. T. Tsumori, S. Yokota, Y. Qin, T. Oka, Y. Yasui, A light and electron microscopic analysis of the convergent insular cortical and amygdaloid projections to the posterior lateral hypothalamus in the rat, with special reference to cardiovascular function. *Neurosci. Res.* **56**, 261–269 (2006).
30. E. A. Grove, Efferent connections of the substantia innominata in the rat. *J. Comp. Neurol.* **277**, 347–364 (1988).
31. H. J. Groenewegen, H. W. Berendse, S. N. Haber, Organization of the output of the ventral striatopallidal system in the rat: Ventral pallidal efferents. *Neuroscience* **57**, 113–142 (1993).
32. E. S. Gurdjian, The diencephalon of the albino rat. Studies on the brain of the rat. No. 2. *J. Comp. Neurol.* **43**, 1–114 (1927).
33. A. Brodal, The amygdaloid nucleus in the rat. *J. Comp. Neurol.* **87**, 1–16 (1947).
34. A. J. McDonald, Cytoarchitecture of the central amygdaloid nucleus of the rat. *J. Comp. Neurol.* **208**, 401–418 (1982).
35. L. W. Swanson, *Brain Architecture: Understanding the Basic Plan*, (Oxford University Press, 2012).
36. J. Kim, X. Zhang, S. Muralidhar, S. A. LeBlanc, S. Tonegawa, Basolateral to central amygdala neural circuits for appetitive behaviors. *Neuron* **93**, 1464–1479.e5 (2017).
37. G. F. Alheid, Extended amygdala and basal forebrain. *Ann. N. Y. Acad. Sci.* **985**, 185–205 (2003).
38. J. Altman, S. A. Bayer, The development of the rat hypothalamus. *Adv. Anat. Embryol. Cell Biol.* **100**, 1–178 (1986).
39. D. M. Martin *et al*., PITX2 is required for normal development of neurons in the mouse subthalamic nucleus and midbrain. *Dev. Biol.* **267**, 93–108 (2004).
40. M. R. Waite *et al*., Pleiotropic and isoform-specific functions for Pitx2 in superior colliculus and hypothalamic neuronal development. *Mol. Cell. Neurosci.* **52**, 128–139 (2013).
41. J. M. Skidmore, J. D. Cramer, J. F. Martin, D. M. Martin, Cre fate mapping reveals lineage specific defects in neuronal migration with loss of Pitx2 function in the developing mouse hypothalamus and subthalamic nucleus. *Mol. Cell. Neurosci.* **37**, 696–707 (2008).
42. M. P. Smidt *et al*., Analysis of three Ptx2 splice variants on transcriptional activity and differential expression pattern in the brain. *J. Neurochem.* **75**, 1818–1825 (2000).
43. C. R. Gerfen, C. J. Wilson, "The basal ganglia" in *Integrated Systems of the CNS, Part III*, (Elsevier, 1996), pp. 371–468.
44. A. Pautrat *et al*., Revealing a novel nociceptive network that links the subthalamic nucleus to pain processing. *eLife* **7**, e36607 (2018).
45. H. J. Groenewegen, H. W. Berendse, Connections of the subthalamic nucleus with ventral striatopallidal parts of the basal ganglia in the rat. *J. Comp. Neurol.* **294**, 607–622 (1990).
46. W. I. A. Haynes, S. N. Haber, The organization of prefrontal-subthalamic inputs in primates provides an anatomical substrate for both functional specificity and integration: Implications for basal ganglia models and deep brain stimulation. *J. Neurosci.* **33**, 4804–4814 (2013).
47. G. Temiz, S. B. Sébille, C. Francois, E. Bardinet, C. Karachi, The anatomo-functional organization of the hyperdirect cortical pathway to the subthalamic area using in vivo structural connectivity imaging in humans. *Brain Struct. Funct.* **225**, 551–565 (2020).
48. S. J. Augood, H. J. Waldvogel, M. C. Münkle, R. L. Faull, P. C. Emson, Localization of calcium-binding proteins and GABA transporter (GAT-1) messenger RNA in the human subthalamic nucleus. *Neuroscience* **88**, 521–534 (1999).
49. K. S. Smith, A. M. Graybiel, A dual operator view of habitual behavior reflecting cortical and striatal dynamics. *Neuron* **79**, 361–374 (2013).
50. D. Z. Jin, N. Fujii, A. M. Graybiel, Neural representation of time in cortico-basal ganglia circuits. *Proc. Natl. Acad. Sci. U.S.A.* **106**, 19156–19161 (2009).
51. A. M. Graybiel, Network-level neuroplasticity in cortico-basal ganglia pathways. *Parkinsonism Relat. Disord.* **10**, 293–296 (2004).
52. A. M. Graybiel, T. Aosaki, A. W. Flaherty, M. Kimura, The basal ganglia and adaptive motor control. *Science* **265**, 1826–1831 (1994).
53. J. R. Schank, M. Heilig, Substance P and the neurokinin-1 receptor: The new CRF. *Int. Rev. Neurobiol.* **136**, 151–175 (2017).
54. L. Sosulina *et al*., Substance P excites GABAergic neurons in the mouse central amygdala through neurokinin 1 receptor activation. *J. Neurophysiol.* **114**, 2500–2508 (2015).
55. G. D. Petrovich, C. A. Ross, P. Mody, P. C. Holland, M. Gallagher, Central, but not basolateral, amygdala is critical for control of feeding by aversive learned cues. *J. Neurosci.* **29**, 15205–15212 (2009).
56. C. A. Campos, A. J. Bowen, C. W. Roman, R. D. Palmiter, Encoding of danger by parabrachial CGRP neurons. *Nature* **555**, 617–622 (2018).
57. J. Y. Chen, C. A. Campos, B. C. Jarvie, R. D. Palmiter, Parabrachial CGRP neurons establish and sustain aversive taste memories. *Neuron* **100**, 891–899.e5 (2018).
58. Y. Shinohara, M. Yamano, T. Matsuzaki, M. Tohyama, Evidences for the coexistence of substance P, neurotensin and calcitonin gene-related peptide in single neurons of the external subdivision of the lateral parabrachial nucleus of the rat. *Brain Res. Bull.* **20**, 257–260 (1988).
59. H. Guo *et al*., Whole-brain monosynaptic inputs to hypoglossal motor neurons in mice. *Neurosci. Bull.*, 10.1007/s12264-020-00468-9 (2020).
60. J. Ciriello, L. P. Solano-Flores, M. P. Rosas-Arellano, G. J. Kirouac, T. Babic, Medullary pathways mediating the parasubthalamic nucleus depressor response. *Am. J. Physiol. Regul. Integr. Comp. Physiol.* **294**, R1276–R1284 (2008).
61. S. Li, G. J. Kirouac, Projections from the paraventricular nucleus of the thalamus to the forebrain, with special emphasis on the extended amygdala. *J. Comp. Neurol.* **506**, 263–287 (2008).
62. G. J. Kirouac, Placing the paraventricular nucleus of the thalamus within the brain circuits that control behavior. *Neurosci. Biobehav. Rev.* **56**, 315–329 (2015).